Supporting Information

Fully textured monolithic perovskite/silicon tandem solar cells with 25.2% power conversion efficiency

Florent Sahli,[1]‡ Jérémie Werner,[1]‡ Brett A. Kamino,[2] Matthias Bräuninger,[1] Raphaël Monnard,[1] Bertrand Paviet-Salomon,[2] Loris Barraud,[2] Laura Ding,[2] Juan J. Diaz Leon,[2] Davide Sacchetto,[2] Gianluca Cattaneo,[2] Matthieu Despeisse,[2] Mathieu Boccard,[1] Sylvain Nicolay,[2] Quentin Jeangros*,[1] Bjoern Niesen,[2] and Christophe Ballif[1,2]*

[1] Ecole Polytechnique Fédérale de Lausanne (EPFL), Institute of Microengineering **(**IMT**)** Photovoltaics and Thin-Film Electronics Laboratory (PV-Lab), Rue de la Maladière 71b, 2002 Neuchâtel, Switzerland.

[2] CSEM, PV-Center, Jaquet-Droz 1, 2002 Neuchâtel, Switzerland.

E-mail: florent.sahli@epfl.ch, quentin.jeangros@epfl.ch

‡ These authors contributed equally.

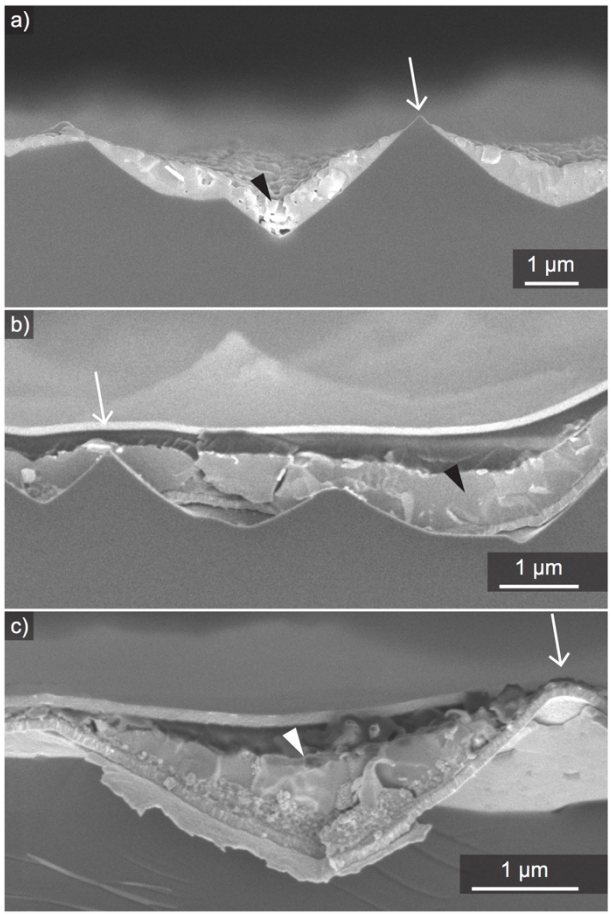

Figure S1: Solution-processed top cells on textured silicon wafers. Secondary electron SEM images of the cross-section of solution-processed a) perovskite layer, b) planar and c) mesoporous perovskite cells on textured c-Si. The perovskite layer was deposited using the 1-step method.[1] The solution-processed layers and contacts, for example TiO_2 in panel c), accumulate within the valleys (arrowheads). Shunts are likely to form at the summits of pyramids, since the perovskite absorber is absent in these regions (arrows).

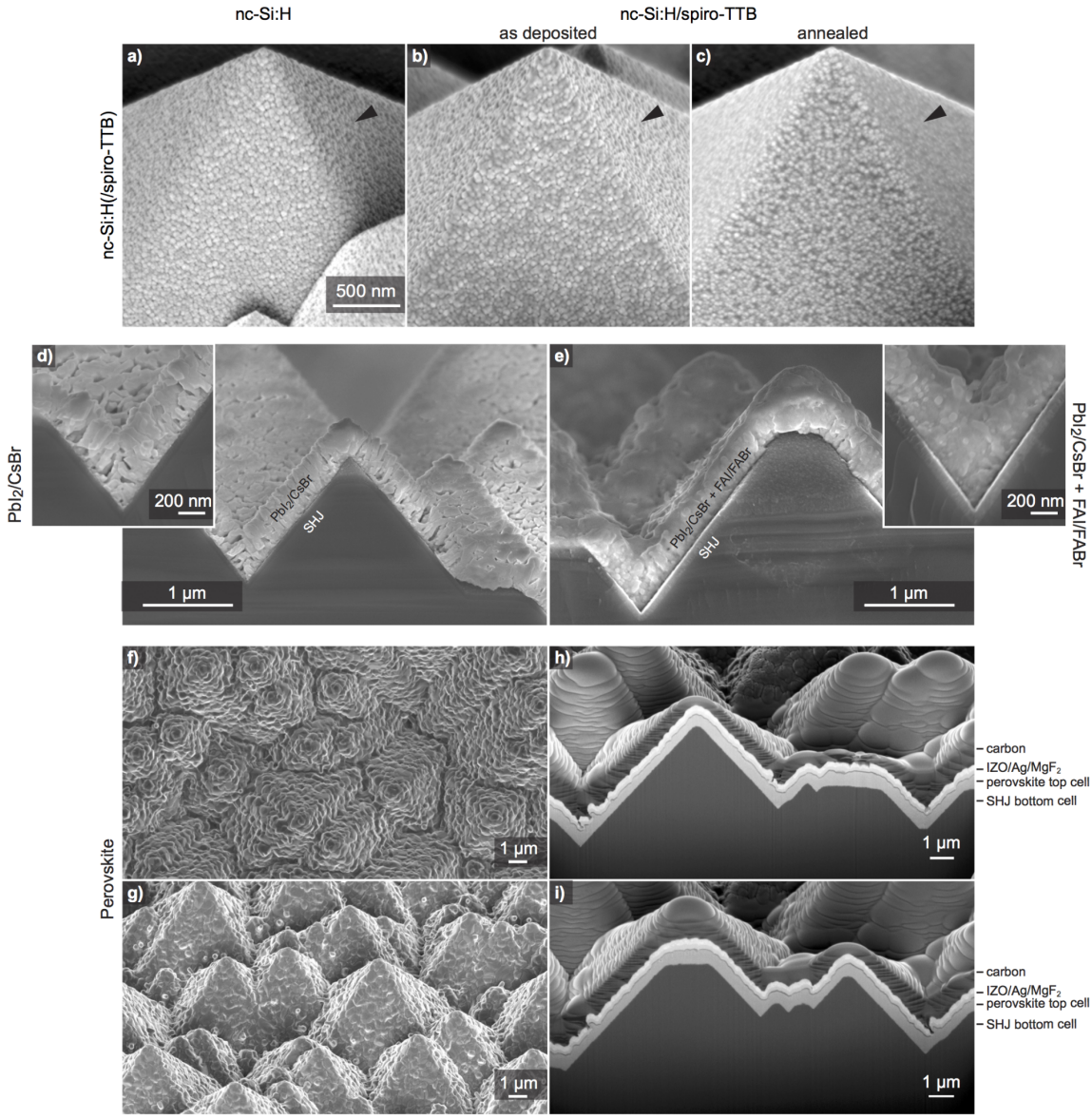

Figure S2: Perovskite top cell fabrication process. a) Secondary electron SEM side view images of the nc-Si:H recombination junction deposited on a fully textured SHJ, b) spiro-TTB as-deposited on this junction and c) the same layer stack after annealing at 150 °C for 30 min to simulate the influence of annealing to crystallize the perovskite. The arrowheads indicate that the spiro-TTB-coated surface appears smoother after annealing when compared to as deposited and the bare nc-Si:H layer; Cross-section SEM images of d) the conformal PbI_2/CsBr template evaporated on the Si pyramids and e) the organohalide solution spin-coated on this PbI_2/CsBr template (before annealing). The left and right insets show magnified views of the bottom of a pyramid valley before and after spin-coating the organohalide solution, respectively; f-g) Top and side view SEM images of the converted perovskite layer after annealing; h-i) FIB-prepared cross-sections, imaged by SEM, of the full perovskite top cell (featuring the full layer stack detailed in Figure 1a).

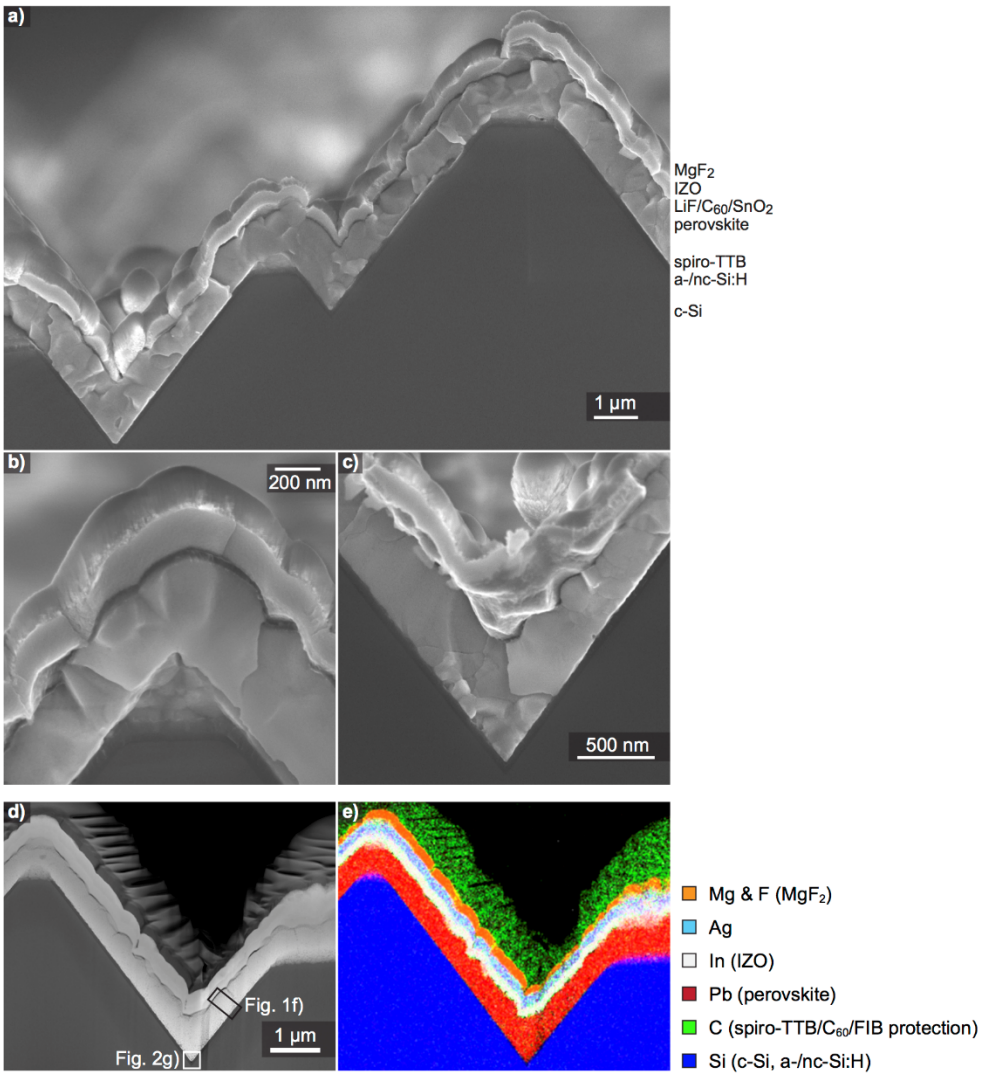

Figure S3: Perovskite top cell microstructure on a textured SHJ bottom cell. Secondary electron cross-section SEM images of the perovskite top cell of a fully textured tandem device (taken in-between grid fingers), showing a) an overview, b) the summit of a pyramid and c) the bottom of a valley; d) STEM high-angle annular dark-field micrograph of the perovskite top cell of a fully textured tandem cell (taken at the position of a grid finger). The positions of the EDX maps shown in Figs. 1f) and 2g) are marked by rectangles; e) Corresponding STEM EDX map of a selection of elements (L ionization edge for Pb, K edges for the other elements).

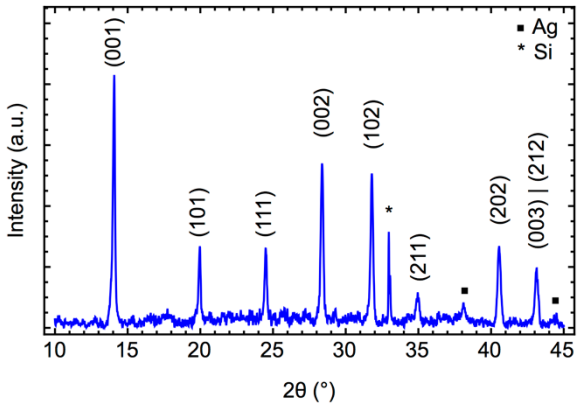

Figure S4: X-ray diffraction pattern of a fully textured perovskite/SHJ tandem after background subtraction. The layers are fully converted, as indicated by the absence of PbI_2 peaks (e.g. the (001) reflection at 12.7°). The Si peak at 33° is the forbidden (002) reflection arising from multiple diffraction.[2]

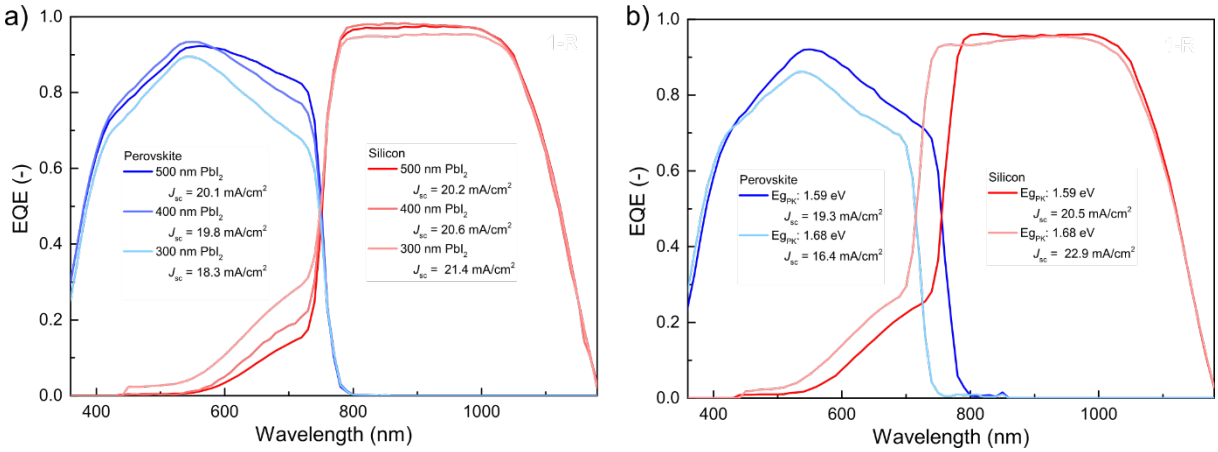

Figure S5: Tandem current matching optimization. a) EQE of fully textured monolithic perovskite/SHJ tandem solar cells with different thicknesses of thermally evaporated PbI_2 (value measured for a flat substrate) with a perovskite bandgap of 1.6 eV. Corresponding thicknesses on the textured SHJ bottom cell are divided by ~ 1.7 due to the geometry of the Si pyramids. The record device was fabricated using 400 nm of thermally evaporated PbI_2, corresponding to ~235 nm of PbI_2 on the c-Si pyramids and leading to a final perovskite thickness on the pyramids of ~440 nm (see Figure 1f); b) EQE of monolithic perovskite/SHJ tandem solar cells featuring two different bandgaps for the perovskite top cell. The respective values are 1.59 eV (dark blue/red) and 1.68 eV (light blue/red).

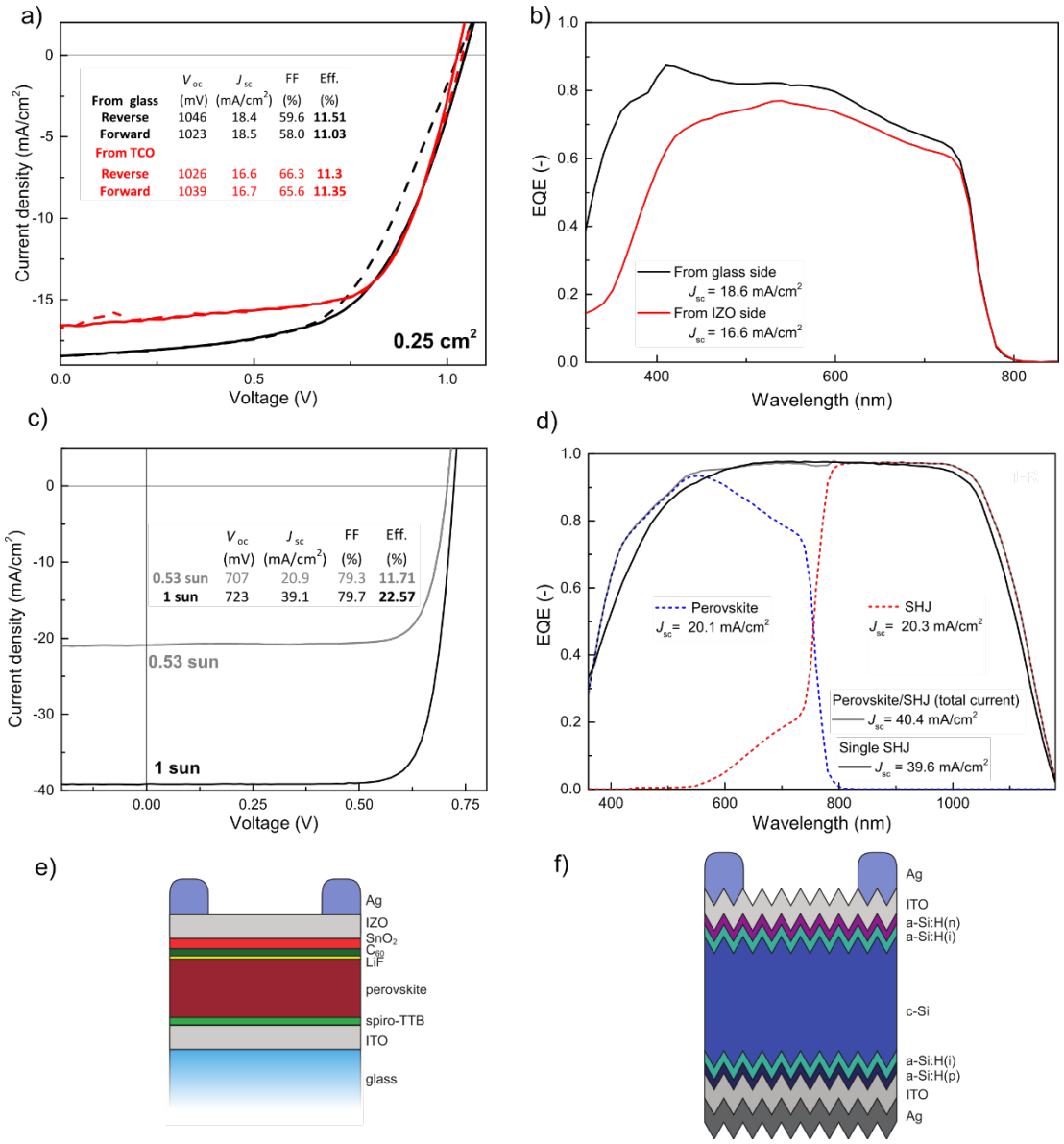

Figure S6: Single-junction performance. a) Semitransparent single-junction perovskite solar cells (0.25 cm^2 aperture area) produced with a similar process sequence as presented for the tandem solar cells. The cell was measured with a scan rate of 100 mV/s; b) Corresponding EQE measured from the glass side (black) or the IZO side (red). The low EQE measured from the film side for the single-junction cell is likely to stem from a higher reflectance at the front surface, resulting from the lack of surface texture, and a higher transparency near the absorption edge due to the thinner perovskite absorber (330 nm in the flat configuration compared to 440 nm for the textured case); c) *J-V* curve of a SHJ bottom cell with 4-cm^2 aperture area; d) Corresponding EQE curve of the SHJ bottom cell alongside the record monolithic fully textured perovskite/SHJ tandem solar cell shown in Figure 4; Schematic views of e) the semitransparent single-junction perovskite solar cell measured in a-b) and f) the silicon heterojunction solar cell (SHJ) measured in c).

a)

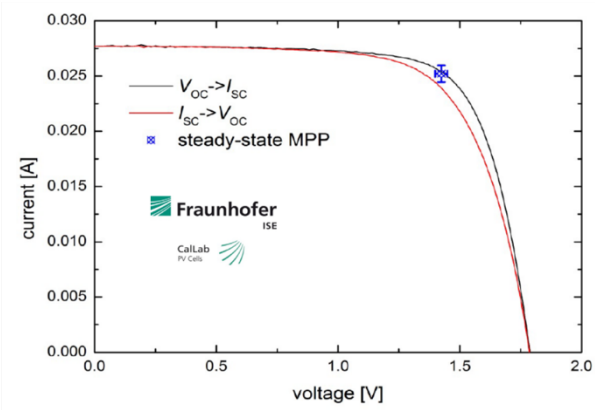

b)

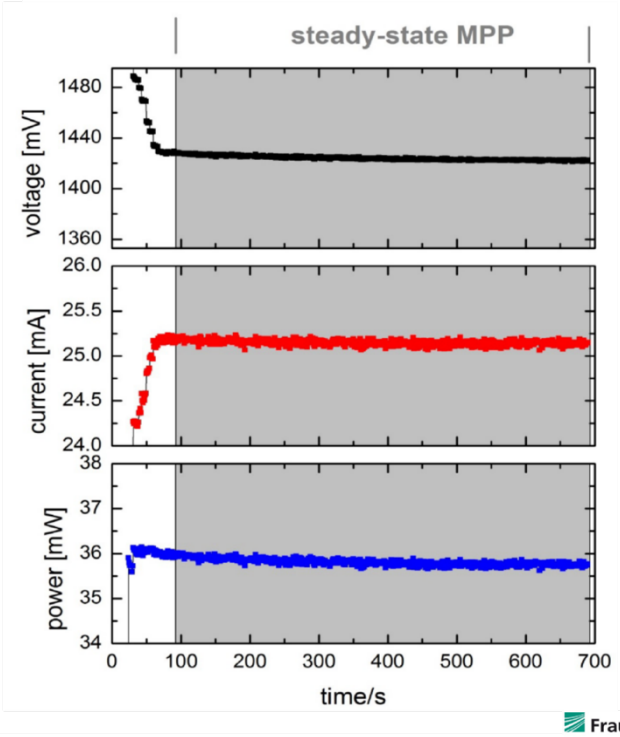

c)

Fraunhofer ISE

CalLab PV Cells

Fläche / *Area* (da)[1]: = (1.419 ± 0.013) cm²

[1] : *(t) = total area, (ap) = aperture area, (da) = designated illumination area /7/*

Kennlinienparameter des Messobjektes unter Standardtestbedingungen (STC) / *IV-curve parameter under Standard Testing Conditions (STC)* :

		Vorwärtsrichtung / *forwards scan direction*		Rückwärtsrichtung / *reverse scan direction*		MPP-Tracking / *MPP-Tracking*	
V_{oc}	=	(1786.0 ± 12.0)	mV	(1788.1 ± 12.0)	mV		
I_{SC} (Ed.2 - 2008)	=	(27.71 ± 0.53)	mA	(27.72 ± 0.53)	mA		
I_{MPP}	=	24.66	mA	25.03	mA	(25.15 ± 0.76)	mA
V_{MPP}	=	1386.0	mV	1446.5	mV	(1424.1 ± 25.0)	mV
P_{MPP}	=	34.18	mW	36.21	mW	(35.81 ± 0.96)	mW
FF	=	69.06	%	73.06	%		
η	=	24.09	%	25.52	%	(25.24 ± 0.72)	%

Figure S7: Certification report. a) Certified *J-V* curves of the 25.24%-efficient monolithic textured perovskite/SHJ tandem solar cell measured with a scan rate of 100 mV/s; b) Voltage (black), current (red), power (blue) during 700 s MPP tracking; c) Corresponding *J-V* and MPP parameters recorded by CalLab, Fraunhofer ISE (1.419 cm^2 aperture area).

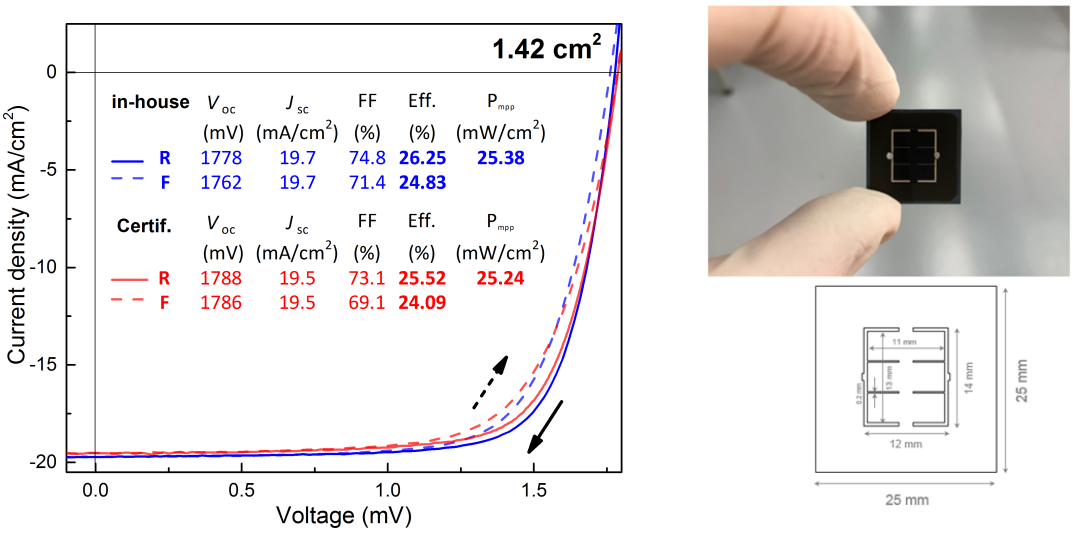

Figure S8: In-house-measured *J-V* characteristics of the record cell. The left panel shows the *J-V* measurements of our best monolithic textured perovskite/SHJ tandem solar cell measured in-house (blue lines) and by CalLab, Fraunhofer ISE (red lines), scanned in the reverse (solid line) and forward (dashed line) directions. It is worth to mention that the certification *J-V* measurements have been carried out ~4 weeks after our in-house *J-V* measurements. All *J-V* measurements were recorded with a scan rate of 100 mV/s; The right panel shows a picture of a 1.42 cm^2 monolithic perovskite/silicon tandem solar cell (top image) and a drawing of the cell design (bottom image).

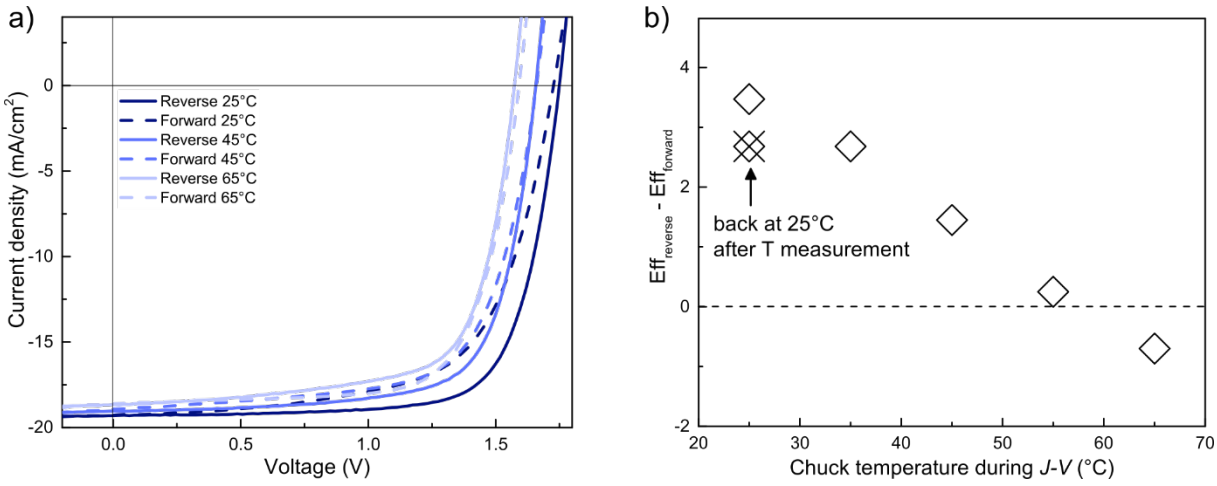

Figure S9: Thermal behavior of the electrical properties of a perovskite/SHJ tandem. a) Temperature-dependent *J-V* measurements of a monolithic textured perovskite/SHJ tandem solar cell, scanned in reverse (solid line) and forward (dashed line) conditions. All *J-V* measurements were recorded with a scan rate of 100 mV/s; b) Difference in efficiency between reverse and forward directions, ($Eff_{reverse} - Eff_{forward}$) as a function of the cell temperature.

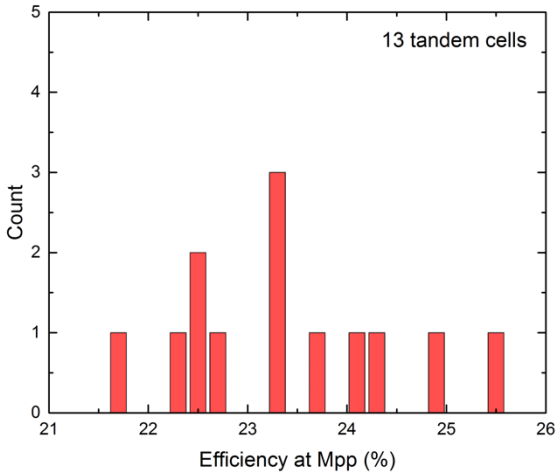

Figure S10: Tandem cell results statistics. Steady-state efficiency from in-house MPP tracking (> 300 s) of a batch of 13 co-processed monolithic textured perovskite/SHJ tandem solar cells.

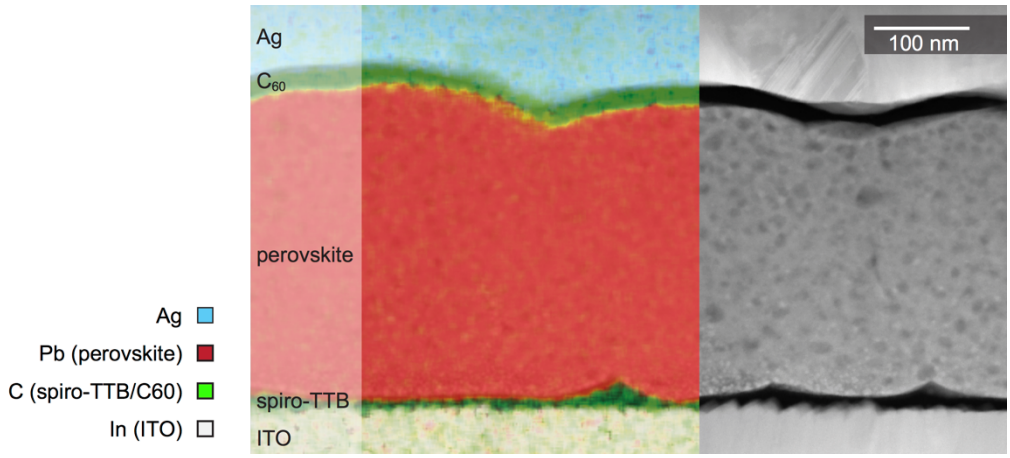

Figure S11: Microstructure of a perovskite single-junction solar cell on a flat substrate. STEM EDX map of selected elements (colored left panel) and corresponding high-angle annular dark-field image (grayscale right panel) of a perovskite single-junction cell deposited on ITO. The spiro-TTB layer remains conformal in a flat configuration. The variations in contrast observed within the perovskite absorber are due to the formation of Pb-rich domains during the FIB sample preparation process.[3,4]

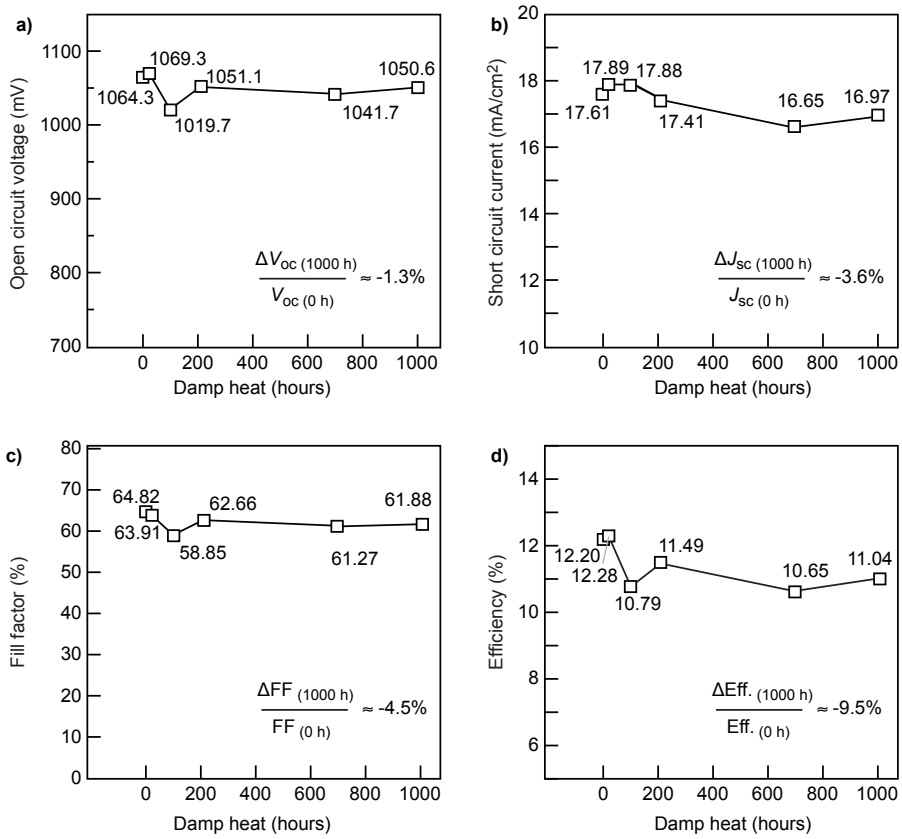

Figure S12: Damp heat test on a semitransparent perovskite solar cell. a-d) Evolution of the photovoltaic characteristics during damp heat stability testing (85 °C in a relative humidity level of 85 % for 1000 hours) of an encapsulated planar single-junction perovskite device (glass/glass with edge sealant). The single-junction perovskite solar cell presented here passes damp heat testing, with <10% relative efficiency drop after 1000 hours.

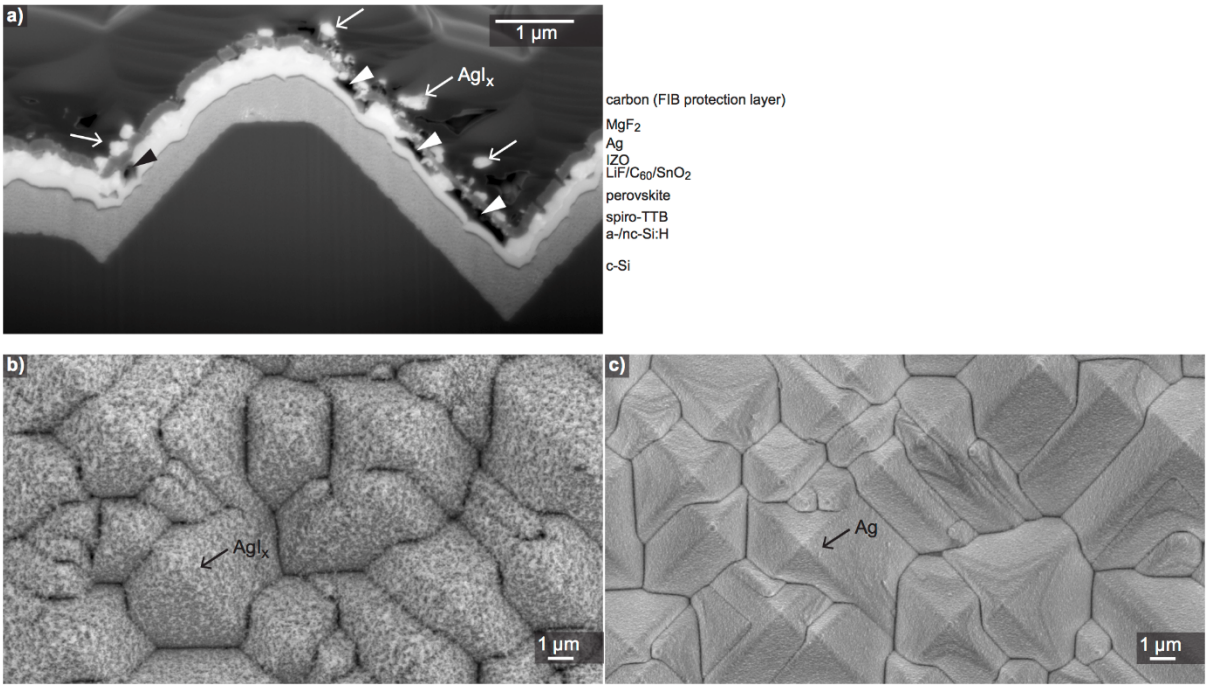

Figure S13: Silver halide formation during light soaking. a) SEM image of a FIB-prepared cross-section prepared at the position of one Ag front finger after the light soaking experiment shown in Figure 5a-b. AgI_x clusters form on the front MgF_2 surface (indicated by arrows), leaving voids at the initial position of the Ag layer (arrowheads), see Figures 1e and S2h-i for a comparison with the initial state; SEM top view images taken at the back of the encapsulated device degraded in Figure 5c-d, showing b) regions of the Ag back metallization that was exposed to a source of iodine with which it reacted, giving rise to an inhomogeneous topography (region close to one conductive ribbon) and c) the Ag back metallization that remained intact below the back conductive ribbon.

References

1. Heo, J. H. *et al.* Efficient inorganic–organic hybrid heterojunction solar cells containing perovskite compound and polymeric hole conductors. *Nat. Photonics* **7,** 486–491 (2013).
2. Zaumseil, P. High-resolution characterization of the forbidden Si 200 and Si 222 reflections. *J. Appl. Crystallogr.* **48,** 528–532 (2015).
3. Srot, V., Gec, M., van Aken, P. A., Jeon, J. H. & Čeh, M. Influence of TEM specimen preparation on chemical composition of Pb(Mg1/3Nb2/3)O3-PbTiO3 single crystals. *Micron* **62,** 37–42 (2014).
4. Jeangros, Q. *et al.* In situ TEM analysis of organic-inorganic metal-halide perovskite solar cells under electrical bias. *Nano Lett.* **16,** 7013–7018 (2016).